NDUFS6 mutations are a novel cause of lethal neonatal mitochondrial complex I deficiency

Denise M. Kirby,[1,2,3] Renato Salemi,[1] Canny Sugiana,[1,3] Akira Ohtake,[4] Lee Parry,[1] Katrina M. Bell,[1] Edwin P. Kirk,[5] Avihu Boneh,[1,2,3] Robert W. Taylor,[6] Hans-Henrik M. Dahl,[1,3] Michael T. Ryan,[4] and David R. Thorburn[1,2,3]

[1]Murdoch Childrens Research Institute and [2]Genetic Health Services Victoria, Royal Children's Hospital, Melbourne, Victoria, Australia. [3]Department of Paediatrics, University of Melbourne, Melbourne, Victoria, Australia. [4]Department of Biochemistry, LaTrobe University, Melbourne, Victoria, Australia. [5]Department of Medical Genetics, Sydney Children's Hospital, Sydney, New South Wales, Australia. [6]Mitochondrial Research Group, School of Neurology, Neurobiology and Psychiatry, University of Newcastle upon Tyne, Newcastle upon Tyne, United Kingdom.

Complex I deficiency, the most common respiratory chain defect, is genetically heterogeneous: mutations in 8 nuclear and 7 mitochondrial DNA genes encoding complex I subunits have been described. However, these genes account for disease in only a minority of complex I–deficient patients. We investigated whether there may be an unknown common gene by performing functional complementation analysis of cell lines from 10 unrelated patients. Two of the patients were found to have mitochondrial DNA mutations. The other 8 represented 7 different (nuclear) complementation groups, all but 1 of which showed abnormalities of complex I assembly. It is thus unlikely that any one unknown gene accounts for a large proportion of complex I cases. The 2 patients sharing a nuclear complementation group had a similar abnormal complex I assembly profile and were studied further by homozygosity mapping, chromosome transfers, and microarray expression analysis. *NDUFS6*, a complex I subunit gene not previously associated with complex I deficiency, was grossly underexpressed in the 2 patient cell lines. Both patients had homozygous mutations in this gene, one causing a splicing abnormality and the other a large deletion. This integrated approach to gene identification offers promise for identifying other unknown causes of respiratory chain disorders.

Introduction

Respiratory chain complex I deficiency is the most common disorder of energy generation. It has a wide range of clinical presentations, including lethal infantile mitochondrial disease, Leigh disease and other encephalopathies, cardiomyopathy, myopathy, and liver disease (1–3). Complex I has at least 45 subunits (4, 5), and mutations causing complex I deficiency have been identified in 8 nuclear genes (*NDUFS1*, *NDUFS2*, *NDUFS3*, *NDUFS4*, *NDUFS7*, *NDUFS8*, *NDUFV1*, and *NDUFV2*) (6–13) and 7 mitochondrial DNA (mtDNA) genes (2, 14, 15). These 15 genes encode all the 14 core complex I subunits with prokaryotic counterparts (4, 5) plus a "supernumerary" subunit, NDUFS4, which appears to be involved in regulation of complex I activity by reversible phosphorylation (16). Fewer than 30 families have been described as having mutations in the 8 nuclear genes shown to cause complex I deficiency, and they appear to account for only approximately 20% of patients (6). Mutations in mtDNA also appear to account for approximately 20% of complex I deficiency (14, 15), so the molecular basis remains obscure in the majority of patients.

Complex I deficiency could potentially be caused by mutations in any of the other approximately 30 supernumerary subunit genes (4, 5), in which mutations have not yet been described. In principle, it is possible to investigate all these genes by mutation analysis of a large number of patients. However, experience with other respiratory chain defects such as complex IV deficiency (17) suggests that defects may be more likely in genes involved in expression of mtDNA-encoded subunits or in processing and assembly of subunits into the mature complex. There are few obvious candidate genes in these categories, partly because complex I is not expressed in *Saccharomyces cerevisiae*, and the lack of yeast mutants makes our understanding of complex I assembly relatively weak. Two assembly factors for complex I have been identified in *Neurospora crassa* (18), and the gene for the human homologue of one, *CIA30*, has been cloned, but no patients with *CIA30* mutations have been found (19). It is likely that mutations in genes for as-yet-undiscovered complex I assembly, import, or expression factors will cause complex I deficiency, but we do not at present know whether there is likely to be a large or small number of unknown causes of complex I deficiency.

Complementation analysis has proven to be a powerful tool to characterize genetic heterogeneity of at least two other organellar disorders. A common complementation group was identified in peroxisomal biogenesis disorders (20) and in respiratory chain complex IV deficiency (21, 22). In both these examples, identification of several unrelated patients within individual complementation groups facilitated subsequent identification of the causative genes, *PEX1* (23, 24) and *SURF1* (25, 26), by somatic cell genetic, genomic, or candidate gene studies.

Complementation analysis has not been reported for complex I deficiency. We investigated whether an unrecognized gene may be a common cause of complex I deficiency using a strategy that involved

Nonstandard abbreviations used: BN-PAGE, Blue Native PAGE; CS, citrate synthase; MMCT, microcell-mediated chromosome transfer; mtDNA, mitochondrial DNA.

Conflict of interest: The authors have declared that no conflict of interest exists.

Citation for this article: *J. Clin. Invest.* **114**:837–845 (2004). doi:10.1172/JCI200420683.

Table 1
Clinical presentation, blood lactate, age of onset and death (if applicable), and residual complex I activity in primary fibroblasts of the 10 patients included in the complementation study

Patient	M/F	Clinical presentation	Blood lactate (normal: <2.5 mM)	Age of onset	Age at death	% CoI/CS in fibroblasts (normal range: 50–137%)
A[A]	M	LIMD	19.2	Neonatal	7 d	25
A2[A]	F		NA	PND		2
A3[A]	M		NA	PND		11
B[B]	M	LIMD	12.0	Neonatal	6 d	7
C	F	LIMD	6.4	Neonatal	11 d	4
C2	F	LIMD	6.7	Neonatal	6 d	NA
D	F	LIMD	6.8	6 wk	6 mo	1
E	F	LD	7.0	9 mo	3 yr 9 mo	14
F	M	LIMD	5.8	Neonatal	4 mo	14
G[C]	M	Myopathy	NT	Adult	Alive as adults	<1
G2[C]	M		NT	Adult	Alive as adults	<1
H	M	LD	11.0	Neonatal	Alive at 15 yr	11
I	M	Persistent LA and FTT	64.3	Neonatal	2 yr 4 mo	17
J	F	LD-like	2.1	2 yr	Alive at 13 yr	19

LIMD, lethal infantile mitochondrial disease; LD, Leigh disease; NT, not tested; LA, lactic acidosis; FTT, failure to thrive; PND, prenatal diagnosis, affected fetus terminated; M, male; F, female; NA, not available; CoI/CS, complex I activity relative to CS activity expressed as percentage of mean of 35 controls (2). [A]Patient A was the first child of first-cousin parents. Prenatal diagnosis by enzyme analysis of cultured chorionic villi revealed complex I deficiency in 2 of 4 subsequent pregnancies. Complex I deficiency was confirmed in fibroblasts after termination of pregnancy (A2 and A3). [B]Consanguineous parents. [C]Patients G and G2 were brothers with adult-onset myopathy who expressed a severe complex I defect in fibroblasts.

pairwise fusion of 10 patient cell lines expressing different antibiotic resistance genes, isolation of heterokaryons by selection with both antibiotics, and assay of complex I activity to determine whether it was rescued (complemented). DNA from the 10 patients had previously been screened by denaturing HPLC to exclude mutations in 6 of the 8 nuclear subunit genes known to cause complex I deficiency. We show it is unlikely that a single major unidentified causative gene exists and identify a novel genetic cause of complex I deficiency.

Results

Complementation analysis. Ten patients whose complex I deficiency was expressed in cultured fibroblasts (Table 1) were studied. Results of screening for mutations in the 6 nuclear complex I subunit genes first shown to cause complex I deficiency (*NDUFS1*, *NDUFS2*, *NDUFS4*, *NDUFS7*, *NDUFS8*, and *NDUFV1)* and for mtDNA mutations previously associated with complex I deficiency were negative.

The results of all cell fusion experiments are summarized in Table 2, divided into three categories: those with less than 30% normal complex I activity, i.e., not complemented; those between 30% and 50% activity, i.e., intermediate activity; and those with greater than 50% activity, which we considered complemented. We chose 30% as a cut-off figure for lack of complementation because our diagnostic scheme defines residual enzyme activity less than 30% in cultured cells as a major criterion for diagnosis of a respiratory chain defect (27). The 30–50% intermediate category is somewhat arbitrary; however, post hoc analysis suggests that this is reasonable. Mean complex I activity in patient-patient hybrids — excluding those involving (a) 3 patients (D, E, and J) in whom an mtDNA cause was suggested by fusions with the ρ^0 cell line, which contains no detectable mtDNA, (b) sibling pairs A and G, and (c) patients B and C, who did not complement — was 96%, with an SD of 25% (n = 20). The range (± 2 SDs) was 46–146%.

Figure 1 shows results of representative fusion experiments. Fusion of cell lines from 2 affected siblings (patients G and G2) showed no complementation, indicating a defect in the same gene, as expected (Figure 1A). Fusion with a control cell line or the ρ^0 cell line (which lacks mtDNA) resulted in complementation, indicating that the defect is caused by a nuclear gene showing autosomal recessive inheritance (28).

Figure 1B shows results of fusions of cell lines from unrelated patients A and B, both with consanguineous parents. The patient cell lines clearly complemented each other and were complemented by the ρ^0 cell line, indicating that they have defects in different genes and confirming the nuclear origin of these defects. Figure 1C shows results of fusions of cell lines from unrelated patients B and C. These 2 patient cell lines showed no complementation but were both complemented by the ρ^0 cell line, indicating that they have a defect in the same nuclear gene. Finally, the results of fusions of cell lines from unrelated patients D and E are shown in Figure 1D. These 2 patient cell lines showed no complementation and were not complemented by the ρ^0 cell line, indicating that they both have a defect in mtDNA.

Fusions between patient cell lines and ρ^0 cells resulted in complete restoration of complex I activity (93–156%) for 7 of the 10 patients. Two pairs of unrelated patient cell lines (B and C, D and E) failed to complement each other (15% and 18% complex I activity in fusions, respectively), which suggests that, for each pair, a mutation in the same gene was causative. For 3 patients (D, E, and J), an mtDNA etiology was suggested by the absence of phenotypic rescue in hybrids with a ρ^0 cell line that lacked mtDNA.

Mitochondrial DNA analysis. Complete mtDNA genome sequence analysis in patients D and E identified the same novel pathogenic mutation in both patients, a T10158C transition in the *MTND3* subunit gene of complex I, predicting a serine-to-proline substitution, as described elsewhere (15).

Complete mtDNA sequence analysis in patient J, who was of Polynesian origin, identified 3 changes that may have been pathogenic: G10197A in the *MTND3* subunit gene of complex I, C12239T in the *MTTS2*, and A15746G in the *MTCYB* gene. These changes had not been reported as polymorphic variants in the Mitomap database (Mitomap: A Human Mitochondrial Genome Database, http://www.mitomap.org/). However, screening of DNA samples from 21 other Polynesian patients showed that all 3 variants were consistently present in all samples with the most common Polynesian haplotype (group I, haplotype 11) (29) (not shown). These variants are thus neutral polymorphisms, and mtDNA sequencing essentially excludes the presence of a pathogenic mtDNA mutation in patient J. Patient J had intermediate results for complex I activity in several fusions, including that with the ρ^0 cell line (Table 2). We postulate that patient J may

Table 2
Summary of complementation results

	N	A	B	C	D	E	F	G	H	I	J	ρ⁰
N	100	93	93	85	76	88	101	87	94	86	75	93
A		46	83	81	106	116	105	85	126	114	64	157
B				**15**	157	62	98	149	121	74	36	152
C					36	73	87	117	98	61	70	144
D						**18**	95	84	95	78	30	**28**
E							55	68	110	42	39	36
F								96	119	57	75	139
G								**19**	73	67	83	94
H										119	57	109
I											39	151
J												32

Complex I activity is expressed relative to the activity of the matrix marker enzyme CS (CoI/CS), as percentage of the mean of the fusions of each of the 2 parental cell lines for each fusion with the control cell line, e.g., for the fusion of cell lines from patients A and B, CoI/CS in the hybrids between patients A and B is expressed as the percentage of the mean of the CoI/CS in the fusions of cell lines from patient A with the control and patient B with the control. Boldface text: CoI/CS < 30%; underlined text: CoI/CS 30–50%. N, control cell line.

have an autosomal dominant cause for complex I deficiency. She has a de novo translocation between chromosomes 11 and 18, and studies are underway to define the breakpoints and identify a putative causative gene. However, there are no complex I subunit genes or obvious candidate genes on either chromosome in the breakpoint regions as defined so far.

Complex I assembly. The amount and size of assembled complex I in patient cell lines was analyzed by Blue Native PAGE (BN-PAGE) immunoblotting. Complex I in the normal cell line is mainly about 900 kDa with some super-complexes, presumably consisting of complex I, complex III, and complex IV, also visible (30). Patients A, G, and I had almost undetectable levels of fully assembled complex I (~5% of control), and patients F and H had severely reduced levels (~20%). Patients D and E, with the mtDNA T10158C mutation, and patient J had relatively normal levels of fully assembled complex I (60–75%). Patients B and C, who are in the same nuclear complementation group, also had normal total amounts of complex I protein. However, the amount of fully assembled 900-kDa complex was decreased, and most of the complex (64%) was present in a unique complex of about 750 kDa not seen in other patients (Figure 2B). This is further evidence that the same gene is causing complex I deficiency in both patients and that the defect results in incomplete assembly.

Homozygosity mapping. Patient B was the only child of consanguineous (first cousin) Australian parents (Figure 3A). Patients C and C2 were the daughters of Turkish parents who were not known to be consanguineous but were from the same small village (population approximately 200). There were several unexplained infant deaths in relatives, and consanguinity was documented in one branch of the family (Figure 3B), which suggests that the parents were likely to be carriers of the same mutant allele inherited from a common ancestor. Families B and C were expected to have different mutations in the same gene, and each of the 3 patients was expected to be "homozygous by state" for polymorphic markers near the causative gene.

A 5-cM genome-wide scan identified 38 of 811 markers as being homozygous in all 3 affected individuals (Figure 4). We focused initially on potentially the largest regions of homozygosity, represented by 3 adjacent homozygous markers on chromosome 2p and 2 adjacent homozygous markers on chromosomes 2q and 21p. The 2p region contained a strong candidate gene, *HIRIP5*, potentially involved in mitochondrial iron-sulfur metabolism (31), but no mutations were identified in either patient by sequencing the 8 exons and flanking regions of *HIRIP5* genomic DNA. Fine mapping narrowed the 13.3-Mb homozygous region on 2p to a 5.4-Mb region between markers D2S2320 and D2S101 and downgraded the significance of the 2q and 21p regions by identifying intervening heterozygous markers. Microcell-mediated chromosome transfer (MMCT) using a hybrid rodent cell line containing human chromosome 2 as a donor failed to correct the complex I defect in fibroblasts from patient B. All 22 MMCT clones analyzed showed deficient complex I activity (<10% residual activity), which excluded chromosome 2 as encoding the causative gene in these families. We then used two independent approaches to investigate other homozygous regions throughout the genome.

Figure 1
Representative fusions of individual patient cell lines and of patient cell lines and a ρ⁰ (r0) cell line (lacking mtDNA) and a control cell line. Results are shown as complex I activity relative to the mitochondrial matrix marker enzyme CS, as percentage of the mean of fusions between control cell lines (observed range for complex I activity relative to CS activity: 164–169, $n = 2$ fusions). Error bars represent the observed range for all values for each cell line. N, transformed control fibroblasts; ρ⁰, transformed 143BTK⁻ρ⁰ osteosarcoma cell line; A, B, C, D, E, and G, complex I–deficient transformed fibroblasts from patients A–G; others, hybrids between the parental cell lines as indicated. For the parental cell lines, the mean and observed ranges for the G418-resistant and hygromycin B–resistant lines combined are shown. Number of estimations for each cell line were: N, $n = 23$; ρ⁰, A, and C, $n = 8$; B, $n = 11$; D, $n = 14$; E, $n = 9$; G, $n = 7$; G2, $n = 1$; A × B, B × ρ⁰, A × N, C × ρ⁰, D × ρ⁰, E × N, G × G2, G × ρ⁰, and G × N, $n = 2$; A × ρ⁰, $n = 3$; B × C, C × N, D × N, and E × ρ⁰, $n = 4$; D × E, $n = 6$; B × N, $n = 8$. (**A**) Affected brothers G and G2 are in the same (nuclear) complementation group. (**B**) Patients A and B represent 2 different (nuclear) complementation groups. (**C**) Patients B and C represent the same (nuclear) complementation group. (**D**) Patients D and E represent the same (mtDNA) complementation group.

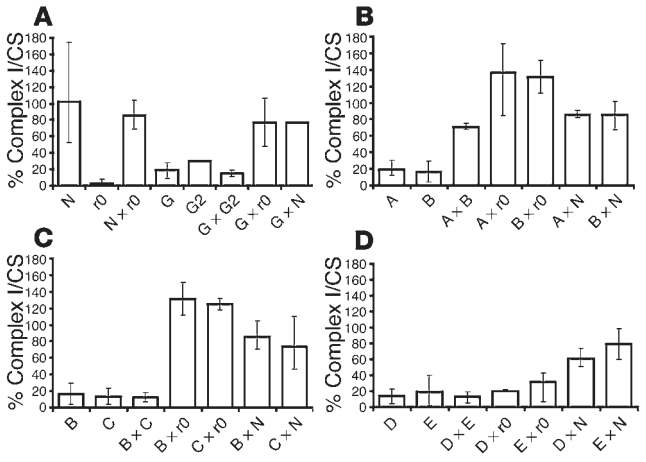

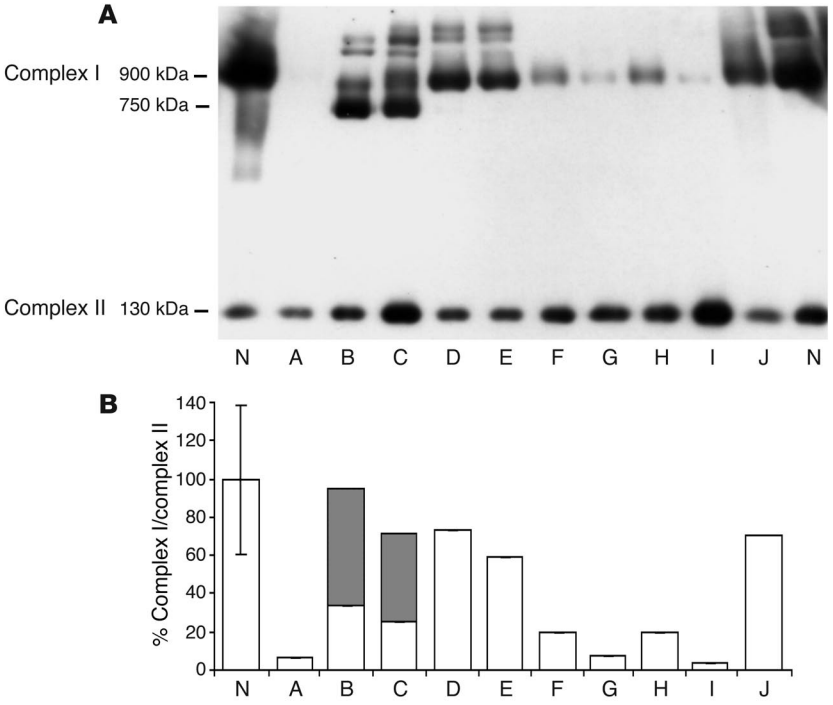

Figure 2
Immunoblot analysis and quantitation of complexes I and II from fibroblasts of patients A–J and controls (N) following separation by BN-PAGE. (**A**) Fully assembled complex I detected by an antibody to the 39-kDa subunit is at approximately 900 kDa. Partially assembled complex I detected by the same antibody is at approximately 750 kDa, and fully assembled complex II detected by an antibody to the 70-kDa subunit is at approximately 130 kDa. (**B**) Histogram showing percentage fully (white bars) and partially (gray bars) assembled complex I relative to fully assembled complex II in primary fibroblasts. The error bar represents the observed range for 2 different control cell lines.

Complex I subunit genes. First, we compared the chromosomal locations of all complex I subunit genes with the homozygous markers. Eight subunit genes were adjacent to homozygous markers from the 5-cM genome-wide scan, but fine mapping excluded four of these as being in homozygous regions. Of the remaining 4 candidate subunit genes, *NDUFV1* and *NDUFS8* on chromosome 11 had previously been excluded by mutation screening. The X chromosomal location of *NDUFA1* meant the marker was actually hemizygous in patient B and was inconsistent with autosomal recessive inheritance. Thus *NDUFS6* on chromosome 5 was the only plausible subunit gene compatible with homozygosity mapping, fine mapping, and previous mutation screening (Figure 4).

Transcriptome analysis. Microarray analysis was used as an alternative approach that could potentially identify genes of known or unknown function with abnormal expression in the patient cell lines, whose location could be compared with the homozygous markers. We used oligonucleotide microarrays representing 17,260 genes from the Compugen 19,000 library to identify differentially expressed genes in cell lines of patients B and C. Seven of the 50 genes showing the most statistically significant differential expression were downregulated in both patients, and these are listed in Table 3. This analysis confirmed *NDUFS6* as an obvious candidate gene, since it was the only gene in close proximity to a homozygous marker from the genome-wide scan that showed marked downregulation in both patient cell lines when analyzed individually or when the data from both cell lines were pooled.

Real-time RT-PCR analysis confirmed that *NDUFS6* mRNA levels (normalized to 18S RNA) were dramatically decreased in patients B and C compared with control. *NDUFS6* expression was undetectable in patient B, in both E6E7-transduced cells and primary fibroblasts, while patient C had only 3% of the control level in both cell lines (Table 4). By contrast, patient A, with an unknown nuclear gene defect, had a 52% decrease in *NDUFS6* expression in E6E7-transduced cells and a 24% increase in primary fibroblasts. These modest changes are too small to be regarded as significant in patient A and provide further support for the specificity of *NDUFS6* underexpression in patients B and C.

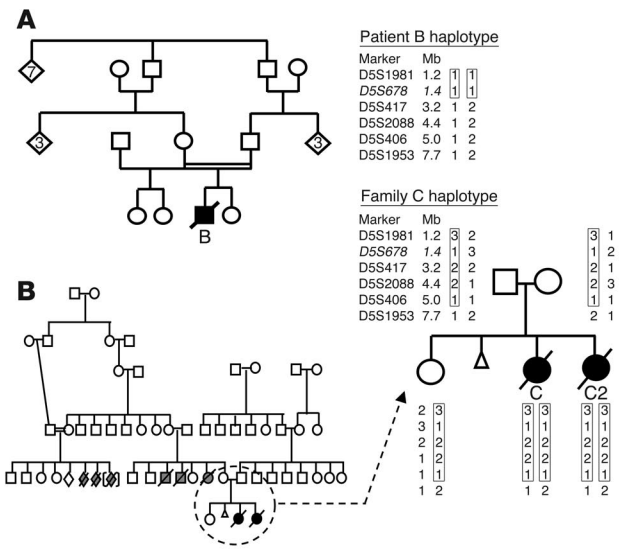

Figure 3
Pedigrees and haplotyping of families B and C. The symbols denote the following: open squares, unaffected males; open circles, unaffected females; open diamonds, an additional number of unaffected siblings; slashed symbols, unexplained infant deaths; triangle, miscarriages; black symbols, affected children. The homozygous regions in the probands are indicated by rectangles. The polymorphic marker shown in italics is not part of the original 5-cM genome-wide scan marker set. (**A**) Family B pedigree and the chromosome 5 haplotype of the affected child. (**B**) Family C pedigree and the chromosome 5 haplotype shared by the affected siblings.

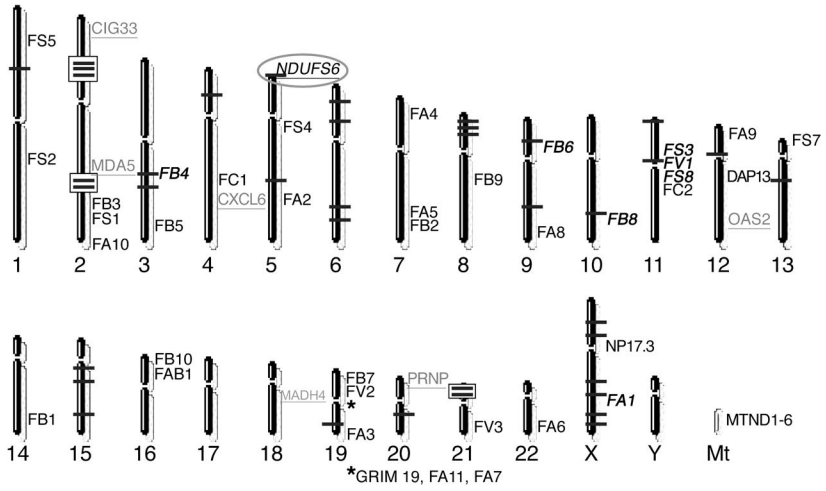

Figure 4
A chromosome map showing the location of markers that were homozygous in all 3 affected children (as horizontal bars) in the initial 5-cM genome-wide scan. Consecutive homozygous markers on chromosomes 2p (D2S2369, D2S337, and D2S2368), 2q (D2S2188 and D2S364), and 21p (D21S1904 and D21S1911) are highlighted by boxes. The approximate locations of all complex I subunit genes are shown in black text, and those subunit genes located adjacent to homozygous regions from the genome-wide scan are shown in bold italicized text. The prefix "NDU" is omitted from subunit gene names for clarity. The locations of the 7 most downregulated genes in both patients compared with control as revealed by microarray analysis are shown by gray underlined text. *NDUFS6* is highlighted by an ellipse, as it was the only subunit gene located adjacent to a homozygous region that showed significant underexpression on microarray analysis.

Mutation analysis of NDUFS6. PCR analysis of *NDUFS6* cDNA amplified a fragment in patient C that was larger than that in control and consistently failed to amplify any fragment in patient B (Figure 5A). Sequencing of *NDUFS6* cDNA and genomic *NDUFS6* exon 2 and adjacent DNA identified the pathogenic mutation in family C. Both affected siblings had a homozygous point mutation (c.186+2T>A) in the splice donor site of exon 2. The ensuing splicing abnormality leads to insertion of 26 bp of intronic material at the exon 2/exon 3 boundary of the cDNA (Figure 5B). This causes a frame shift and creates a premature stop codon predicted to yield a truncated protein of 71 amino acids instead of the wild-type 124 amino acids. The parents and an unaffected sister are heterozygous for this mutation (not shown). The abnormally spliced cDNA could be amplified from RNA of cells grown with cycloheximide, but real-time RT-PCR showed that only 3% of the normal mRNA level was present in cells grown without cycloheximide. This implies that the major effect of this mutation is to cause nonsense-mediated mRNA decay.

Using an approach based on standard PCR in combination with long-range PCR, the *NDUFS6* gene in Family B was found to harbor a 4.175-kb deletion that encompasses exons 3 and 4. *NDUFS6* exons 1 and 2 were successfully amplified from genomic DNA and sequenced in the patient with no mutations identified. However, exons 3 and 4 consistently failed to amplify. With the exon 2 forward primer used as an anchor, reverse primers were designed and staggered at approximately 5-kb intervals downstream of this anchor. A series of long-range PCRs using each reverse primer separately in turn was performed, and a PCR product was generated in the patient with the reverse primer located 15 kb away. The resulting product, however, was only approximately 11 kb in size. This reverse primer was then used as an anchor, and new forward primers were designed at 1-kb intervals, commencing 4-kb upstream to ensure primers were located so that they spanned the deletion. Primers that were expected to yield an approximately 6.2-kb product instead generated an approximately 2.1-kb fragment in the patient (Figure 5C). This product was sequenced, and the deletion breakpoints were precisely identified, with the deletion starting at nucleotide 1,865,286 and extending to nucleotide 1,869,460 on chromosome 5 (UCSC Genome Browser, July 2003 freeze, http://genome.ucsc.edu/cgi-bin/hgGateway) (Figure 5D). The parents of patient B declined DNA testing.

We sequenced *NDUFS6* cDNA and genomic DNA (exon 1) from 22 unrelated complex I–deficient patients of different ethnicities, but no further pathogenic mutations were identified.

Discussion

Functional complementation analysis of 10 unrelated patients with complex I deficiency showed a clear lack of complementation, implying the same gene is defective, in only 2 pairs of patients. The complex I defects in these 10 patients must therefore be caused by mutations in 7 different nuclear genes and 1 mtDNA gene. These patients had been screened for mutations in 6 of the 8 nuclear-encoded complex I subunit genes known to cause complex I deficiency, and no mutations were found. Thus at least 5 of the 7 nuclear genes causing complex I deficiency in our patients must be novel genes. These results indicate it is unlikely that there is a common unidentified gene that will account for a substantial fraction of patients with complex I deficiency. Given the relatively small numbers of patients with mutations in each of the genes known to cause complex I deficiency and the data presented here, there is probably no single gene that accounts for more than about 10% of patients with complex I deficiency.

Five of the 7 nuclear complementation groups identified (represented by patients A, F, G, H, and I) showed gross deficiency of assembled complex I, which suggests possible defects in unidenti-

Table 3
Genes showing the most significant downregulation of expression in both patient B and C cell lines compared with control

Accession number	Symbol	Differential expression (fold change)	B statistic	*P* value
AF026942	*CIG33*	–15.45	11.9	0.0000331
NM_002993	*CXCL6*	–11.31	8.01	0.00311
AF095844	*MDA5*	–7.11	11.1	0.0000875
NM_000311	*PRNP*	–5.03	10.7	0.000146
NM_002535	*OAS2*	–4.89	9.57	0.000555
NM_004553	***NDUFS6***	**–3.97**	**7.33**	**0.00633**
NM_005359	*MADH4*	–3.01	7.17	0.00746

NDUFS6 is shown in bold. The B statistic is an estimate of the posterior log-odds that each gene is differentially expressed (41).

Table 4
Quantitation of *NDUFS6* expression by real-time RT-PCR in E6E7-transduced and primary fibroblasts

Cell Line	$\Delta C_T \pm SD$	*NDUFS6* expression
E6E7 control	9.98 ± 0.33	1.00
E6E7 patient B	25.61 ± 0.10	0.00002
E6E7 patient C	15.03 ± 0.50	0.030
E6E7 patient A	11.03 ± 0.36	0.483
Control	10.92 ± 0.54	1.00
Patient B	22.94 ± 0.33	0.00024
Patient C	16.15 ± 0.44	0.027
Patient A	10.61 ± 0.28	1.238

ΔC_T represents the change in cycle of threshold fluorescence for *NDUFS6* expression relative to the 18S RNA endogenous control for 3–4 replicate samples. *NDUFS6* gene expression in each cell line was normalized by assigning a value of 1 for the control cell line.

fied assembly factors. However, it should be noted that mutations in at least 2 mtDNA-encoded complex I subunit genes, *MTND1* and *MTND6*, cause a similar assembly defect (32, 33), and mutations in some nuclear-encoded subunits could potentially destabilize complex I assembly. Cell lines from patients D and E, with *MTND3* mutations, and patient J showed near-normal amounts of assembled complex I and are thus likely to have defects that primarily affect complex I function, rather than assembly or stability.

Pathogenic mutations in the *NDUFS6* gene have not been described previously. All other nuclear genes that have been shown to cause complex I deficiency encode subunits that are among the 14 most conserved subunits from humans to bacteria (4, 5), with the exception of NDUFS4, which appears to regulate mammalian complex I activity by reversible phosphorylation (16).

While little is known about the role of the NDUFS6 subunit, there seems no doubt that the *NDUFS6* mutations identified here cause complex I deficiency. Complementation analysis predicted that patients B and C would have mutations in the same gene, and they showed a very similar clinical phenotype and a similar abnormal complex I assembly profile. Of 17,260 genes studied by microarray expression analysis, *NDUFS6* was one of the 7 most downregulated genes in both patient cell lines. These findings are explained by the large deletion and splicing abnormality identified in families B and C, respectively, which are expected to generate unstable mRNAs. Furthermore, mutations that affect production of the NDUFS4 subunit have recently been shown to cause an assembly abnormality similar to that seen in our patients (16).

Findings from studies of complex I assembly in *Neurospora crassa* and *Chlamydomonas reinhardtii* mutants (34, 35) suggest that the membrane and peripheral arms of complex I are assembled separately prior to being joined together. The size of the approximately 750-kDa intermediate and the fact it contains the 39-kDa subunit suggest it represents an assembly intermediate of complex I corresponding to the membrane arm accumulated in *N. crassa* and *C. reinhardtii* mutants.

A recent study of human complex I deficient muscle biopsies using 2-dimensional BN-PAGE identified at least 7 different assembly intermediates, some of which contained both peripheral and membrane arm subunits (36). This suggests an alternative model for complex I assembly in mammals, in which the peripheral and membrane arms are not assembled independently. Thus it is unclear whether the approximately 750-kDa intermediate observed in patients B and C represents a simple membrane arm or a more complicated structure. The NDUFS4 and NDUFS6 subunits are both located in the iron-sulfur fraction of complex I. It seems likely that mutations in both subunits are either preventing complete assembly or destabilizing the peripheral arm of complex I. NDUFS6 must play an essential role in complex I biogenesis or stability, since the mutations identified in this study resulted in early and severe clinical manifestations with death in the neonatal period.

To date, most complex I–deficient patients identified with nuclear gene mutations have had "private" mutations, not found in other families, although some recurrent mutations in *MTND* subunits have been identified (2, 14, 15). Given the large number of genes causing complex I deficiency and the paucity of common mutations, it is important to identify methods that may aid in prioritizing which genes to analyze first in an individual patient. BN-PAGE immunoblotting using a single commercially available antibody shows some promise in this regard. It appears that *MTND6* and *MTND1* mutations cause gross deficiency of assembled complex I, *NDUFS4* and *NDUFS6* mutations show accumulation of characteristic assembly intermediates, while *MTND3* and *MTND5* mutations give a relatively normal assembly profile (15, 16, 32, 33). Further discrimination may be possible with BN-PAGE using other antibodies (36) or as more experience is gained with techniques such as microarray analysis.

It is clear that a substantial number of genes causing complex I deficiency remain to be identified. These are likely to include other supernumerary complex I subunits and unknown assembly factors. In the study of inborn errors of metabolism, categorization of patients into common complementation groups provides an advantage for subsequent gene discovery strategies. The combination of functional complementation analysis, assembly analysis, homozygosity mapping, MMCT, bioinformatics, and transcriptome analysis constitutes a powerful approach to the elucidation of the genetic causes of a heterogeneous disease such as complex I deficiency. Families B and C were investigated as a direct consequence of the complementation and protein assembly studies, which led to the identification of a novel cause of complex I deficiency: mutations in the *NDUFS6* complex I subunit gene.

Methods

Patients. This study was approved by the Royal Children's Hospital Ethics in Human Research Committee. Cell lines from 10 patients with severe complex I deficiency expressed in cultured fibroblasts were selected for the complementation study (Table 1). The clinical presentations of 3 patients in whom *NDUFS6* mutations were subsequently identified are summarized below. There was 1 male baby of Anglo-Celtic origin (patient B) and two sibling female babies of Turkish origin (patients C and C2). All 3 were born at term following uneventful pregnancies and were noted to be profoundly hypotonic and drowsy shortly after birth. Abnormal, slowly drifting eye movements, rolling nystagmus, thought to indicate possible seizures, as well as overt seizures occurred on day 1 of life. Patients B and C had no spontaneous movements and minimal response to painful stimuli. Patient C2 made few spontaneous movements but withdrew from painful stimuli. They had weak gag and absent Moro and grasp reflexes and variable (diminished to brisk) deep tendon reflexes. They had a persistent lactic acidosis with high plasma lactate (peak values of 6 to 12 mmol/l). Patient C had hypoglycemia on day 1. Cerebral CT scans of patients C and C2 were normal. Patient C had central hypoventilation and died at

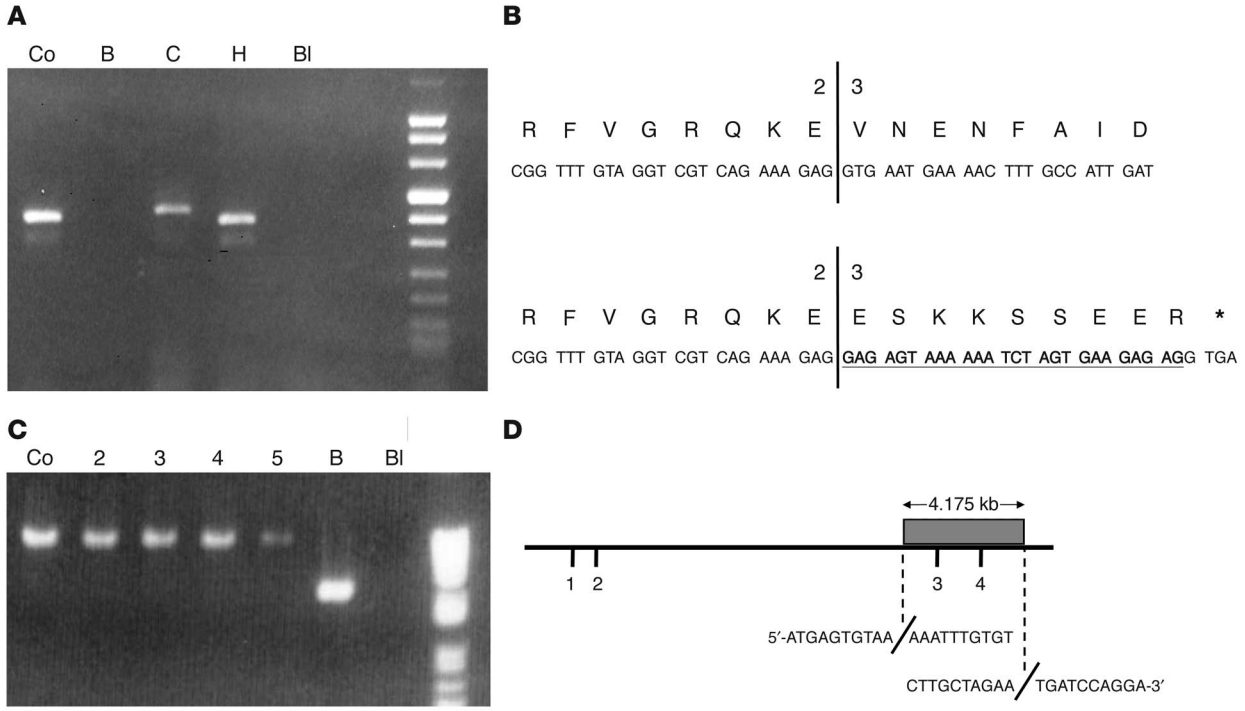

Figure 5
Analysis of *NDUFS6* cDNA and genomic DNA in families B and C. (**A**) Two percent agarose gel of *NDUFS6* cDNA fragments generated by standard PCR. Lanes show control (Co); patient B (B); patient C (C); patient H (H); dH_2O blank (Bl). PCR of *NDUFS6* cDNA gave no product in patient B and a larger fragment than the control in patient C. (**B**) A representation depicting the frameshift and creation of a premature stop codon caused by the 26-bp insertion of intronic sequence in the proband from family C (bottom). Translation of the control sequence is also shown for comparison (top). The diagram shows the exon 2/exon 3 boundary, with the inserted sequence shown in bold and underlined and a stop codon represented by an asterisk. (**C**) 0.8% agarose gel of *NDUFS6* fragments generated by long-range PCR using forward and reverse primers located 6.2 kb apart. Lanes 2–5, unrelated complex I–deficient patients. The PCR product in patient B is approximately 4 kb smaller than that of other samples. The approximately 2-kb fragment from lane 6 was sequenced and the deletion breakpoints elucidated. (**D**) Schematic representation of the 4.175-kb deletion, which encompasses exons 3 and 4 (shaded box) of the 14.5-kb *NDUFS6* gene in the proband from family B. The exact homozygous deletion breakpoints are also shown with the immediate sequence before and after each breakpoint included.

age 11 days. Hypoventilation was noted in patient C2 on day 6, and she died shortly thereafter. Patient B collapsed on day 3 of life and needed assisted ventilation because of hypoventilation. He died on day 6 of life. Neuropathology revealed prominent congestion of the basal ganglia, thalamus, and periventricular tissue of the brain stem. Chromatolysis of many neurons and microvacuolation were present throughout the brain. These findings were similar to those seen in severe hypoxia. The lesions typical of Leigh disease with vascular proliferation, loosening of the neuropil, and preservation of neurons (37) were not seen.

Complex I enzyme and assembly assays, cell culture, and generation of hybrids. Cell culture and assays for complex I and citrate synthase (CS) in mitochondria isolated from patient cell lines, hybrids, and MMCT clones were performed as described (2, 37). Complex I activity was expressed relative to the mitochondrial matrix enzyme CS. The amount and size of assembled complex I were studied by BN-PAGE and immunoblotting using mitochondria isolated from patient cell lines and solubilized with the detergent dodecyl maltoside, as described previously (15, 32).

For complementation analysis, increased growth potential (due to the SV40T antigen) and either G418 resistance or hygromycin B resistance were conferred on patient cell lines and a ρ^0 cell line lacking detectable mtDNA using the plasmids pcDNA3T or pGKHygT, as described (33). Hybrids were generated by fusion with polyethylene glycol and dual antibiotic selection (33). Fusions were set up at least in duplicate and in quadruplicate or more for fusions where initial results suggested lack of complementation or were ambiguous. Complementation was determined by assessing complex I activity in mitochondria isolated from the hybrids.

Microcell-mediated chromosome transfer. Primary fibroblasts from patients and a healthy control were transduced with a retroviral vector expressing the E6E7 region of type 16 human papilloma virus to extend their lifespan (25). A cell line from a panel of human-mouse monochromosomal hybrids (38) was used as the donor of normal human chromosome 2. This chromosome was transferred into the E6E7-transduced patient B cell line by MMCT as described previously (25), except that higher concentrations of colchicine (0.1–0.4 μg/ml) were used to induce micronucleation, and microcells were prepared by centrifugation through a 50% Percoll (Amersham Biosciences) gradient at 32°C and 20,400 g in media containing cytochalasin B (20 μg/ml; Sigma-Aldrich).

Genotyping. Genome-wide scans, fine mapping, and genotyping of hybrids, parental cell lines, and MMCT clones were performed at the Australian Genome Research Facility (Melbourne, Victoria, Australia) using 377 and 3700 DNA sequencers (Applied Biosystems). Data were analyzed with GeneScan Analysis version 3.1.2 and Genotyper version 2.1 software (Applied Biosystems).

Genome-wide scans were performed on purified DNA using the LMS2-HD5 marker set (Applied Biosystems), which has 811 markers spread at an average genetic distance of 5 cM. Mapping of markers additional to those in

the LMS2-HD5 set was also performed. Additional markers used throughout this study were D2S2153, D2S378, D2S2279, D2S2315, D2S1261, D2S2332, D2S2320, D2S402, D2S2397, D2S380, D2S1257, D2S2171, and D2S101 in the 2p region, D2S2173, D2S324, and D2S2261 in the 2q region, and D21S431 in the 21p region. Markers D3S3720, D5S678, D9S43, D10S1133, and D11S1303 were used to characterize homozygous regions adjacent to complex I subunit genes including *NDUFS6*. Hybrids and parental cell lines were genotyped using an AmpFLSTR Profiler PCR Amplification Kit (Applied Biosystems) to confirm that the hybrids contained the expected parental alleles.

Mutation analysis and DNA sequencing. Primary fibroblasts from the 10 patients were grown for 24 hours in 100 μg/ml cycloheximide prior to preparation of RNA in order to minimize nonsense-mediated mRNA decay (39). RNA was reverse-transcribed with Multiscribe reverse transcriptase into cDNA using an RT-PCR kit (Applied Biosystems). cDNA was then screened for mutations in the *NDUFS1*, *NDUFS2*, *NDUFS4*, *NDUFS7*, *NDUFS8*, and *NDUFV1* genes by denaturing HPLC, and no mutations were identified. The method used was essentially as described elsewhere (6), except that a larger number of smaller amplicons for each cDNA were analyzed using a Varian Prostar Helix system. Five amplicons were studied for *NDUFV1*, *NDUFS1*, and *NDUFS2*, 3 amplicons were studied for *NDUFS7* and *NDUFS8*, while 2 amplicons were studied for *NDUFS4*. All patients were also screened for mtDNA mutations shown previously to cause complex I deficiency by sequencing of the *MTTL1* gene and PCR-RFLP analysis of known *MTND* subunit mutations (G3460A, A3796G, and T4160C in *MTND1*; C11777A and G11778A in *MTND4*; T12706C, G13513A and A13514G in *MTND5*; and G14459A in *MTND6*) (15). The entire mtDNA genome of patients D, E, and J was amplified, sequenced, and analyzed as described previously (15, 40).

Automated sequencing for *NDUFS6* was performed on shrimp alkaline phosphatase–treated PCR products (ExoSAP-IT; USB Corp.) using a DYEnamic ET Terminator Cycle Sequencing Kit (Amersham Biosciences). The sequencing reactions were purified using AutoSeq G-50 columns (Amersham Biosciences). Electrophoresis was performed on an Applied Biosystems Prism 3100 Genetic Analyzer at Applied Genetic Diagnostics, University of Melbourne. Sequence data were analyzed using Chromas (Technelysium Pty.) software version 1.51 and compared with the Refseq (http://www.ncbi.nlm.nih.gov/RefSeq/) *NDUFS6* sequence (NM_004553).

The RefSeq *NDUFS6* mRNA sequence contained only a small 5′UTR region, so our forward primer for PCR and sequencing of *NDUFS6* cDNA (GAGAAGGTCACGCACACTGG) lay within exon 1, while the reverse primer (CCCTTTATTCAGCACCAGGA) was within the 3′ UTR. To complete analysis of *NDUFS6*, we also amplified and sequenced exon 1 from genomic DNA of all patients using the primers F1 CCCAGGGCGAAATAAATACC and R1 ATAATCGGCTGCCACAAATC. To characterize the splicing abnormality in patients C and C2, we amplified and sequenced exon 2 and adjacent regions of *NDUFS6* from genomic DNA using primers F2 CTCCAGTTCAGACAGCACCA and R2 TTGTCAGCCTTGACAGCAAC. An Expand Long Template PCR kit (Roche) was used to perform long-range PCR using system 1 buffer/reagent mix and cycling conditions. To generate the approximately 2.1-kb fragment by long-range PCR in patient B, the following primers were used: F GAACAACATAGGTGTGAACT and R ACCTTTTAAGCGCATGGATG. Sequencing primers were: F GAGTGTGCATGAAGGGGACT and R ACACATTTCCCAAGCCAAAG.

Microarrays. Gene expression profiles were obtained by competitive hybridization of patient versus control fibroblast RNA to arrays of the Compugen 19,000 human oligo library Release 1 (Adelaide Microarray Facility, www.microarray.adelaide.edu.au). Over 17,000 human genes are represented on this array, including 34 of the 38 nuclear-encoded complex I subunit genes, the exceptions being the *NDUFA5*, *NDUFS7*, *NDUFV3*, and *NP17.3* genes. Total RNA for analysis was extracted from the E6E7-transduced patient and control fibroblast cell lines grown without cycloheximide and purified using the RNeasy Kit (Qiagen). For analysis, 40 μg of RNA was used to create polyA$^+$ cDNA incorporating an aadUTP [5-(3-aminoallyl)-2′-deoxyuridine 5′-triphosphate sodium salt; Sigma-Aldrich]. cDNA synthesis, dye coupling, hybridization, and washing were performed according to protocols provided by the Adelaide Microarray Facility (http://www.microarray.adelaide.edu.au/protocols/) with the following modifications. For cDNA synthesis, SuperscriptIII (Invitrogen) was used for reverse transcription. Coupling of either a Cy3- or Cy5-CyDye Post-labelling Reactive Dye Pack (Amersham Biosciences) to the cDNA was performed on a QIAquick MinElute purification column (Qiagen). Slides were scanned using a Genepix 4000B scanner (Axon Instruments). The acquired microarray images were analyzed using Genepix Pro 4.0 software (Axon Instruments), and statistical analysis performed using limmaGUI (http://bioinf.wehi.edu.au/limmaGUI/). Data was normalized using Printtip loess normalization within R. Inter-assay variation was determined by label swap experiments, with a total of 4 arrays used for each patient. Microarray data were deposited in MIAME format at www.ebi.ac.uk/arrayexpress/ with accession numbers E-MEXP-118 (patient B data), E-MEXP-119 (patient C data), and A-MEXP-70 (array design).

Real-time RT-PCR. We evaluated *NDUFS6* expression by real-time RT-PCR, using the same total RNA preparations from E6E7 transduced cells that were used in the microarray analyses and total RNA prepared in the same way from the primary fibroblast cell lines. Quantitative expression analysis was performed to determine relative levels of mRNA expression for *NDUFS6* with the use of TaqMan Assay-on-Demand (Applied Biosystems) pre-designed gene expression assay on an ABI Prism 7700 Sequence Detector (Applied Biosystems). The primer and probe sequences along with the optimal conditions for use were predetermined by the manufacturer. A comparative C_T (cycle of threshold fluorescence) method was used with 18S RNA as an endogenous reference and calculations performed per manufacturer's instructions to determine expression of *NDUFS6* in patient cell lines relative to the control cell line. Each sample was run in quadruplicate.

Acknowledgments

The authors thank Lisa Worgan and Michael Buckley for denaturing HPLC screening of complex I subunits, Paige Stevenson and Kelly Ewen-White of the Australian Genome Research Facility for help with genotyping, and Liz Yuen for technical assistance. We acknowledge Michelle DeSilva, Richard Saffery, Nick Wong, and Wendy Hutchison for provision of advice and reagents pertaining to automated sequencing, long-range PCR, and real-time RT-PCR. Denise Galloway and Eric Shoubridge are thanked for providing the E6E7 retroviral packaging cell line. We thank Robert Newbold and Andrew Cuthbert for providing the human chromosome 2/mouse hybrid cell line. John Christodoulou, Maureen Cleary, David Danks, Geoffrey Thompson, Felicity Collins, Janice Fletcher, Graeme Morgan, David Jamison, Barry Lewis, Reuben Matalon, and John Van Hove are thanked for referral of patients and provision of clinical details. This work was supported by grants from the Muscular Dystrophy Association (MDA; USA), the National Health and Medical Research Council (NHMRC; Australia), the Australian Research Council (ARC), the Muscular Dystrophy Campaign (United Kingdom), and the Newcastle upon Tyne Hospitals NHS Trust (United Kingdom). We also acknowledge the Australian Cancer Research Foundation (ACRF) for their support of the Adelaide microarray facility. David R. Thorburn is an NHMRC Senior Research Fellow.

Address correspondence to: David R. Thorburn, Murdoch Childrens Research Institute, Royal Children's Hospital, Flemington Road, Parkville, Victoria 3052, Australia. Phone: 613-8341-6235; Fax: 613-8341-6212; E-mail: david.thorburn@mcri.edu.au.

Denise M. Kirby and Renato Salemi contributed equally to this work.

Akira Ohtake's present address is: Department of Paediatrics, Saitama Medical School, Moroyama Saitama, Japan.

1. Robinson, B.H. 1998. Human complex I deficiency: clinical spectrum and involvement of oxygen free radicals in the pathogenicity of the defect. *Biochim. Biophys. Acta.* **1364**:271–286.
2. Kirby, D.M., et al. 1999. Respiratory chain complex I deficiency: an underdiagnosed energy generation disorder. *Neurology.* **52**:1255–1264.
3. Loeffen, J.L., et al. 2000. Isolated complex I deficiency in children: clinical, biochemical and genetic aspects. *Hum. Mutat.* **15**:123–134.
4. Carroll, J., Fearnley, I.M., Shannon, R.J., Hirst, J., and Walker, J.E. 2003. Analysis of the subunit composition of complex I from bovine heart mitochondria. *Mol. Cell. Proteomics.* **2**:117–126.
5. Murray, J., et al. 2003. The subunit composition of the human NADH dehydrogenase obtained by rapid one-step immunopurification. *J. Biol. Chem.* **278**:13619–13622.
6. Benit, P., et al. 2001. Large-scale deletion and point mutations of the nuclear NDUFV1 and NDUFS1 genes in mitochondrial complex I deficiency. *Am. J. Hum. Genet.* **68**:1344–1352.
7. Loeffen, J., et al. 2001. Mutations in the complex I NDUFS2 gene of patients with cardiomyopathy and encephalomyopathy. *Ann. Neurol.* **49**:195–201.
8. Benit, P., et al. 2004. Mutant NDUFS3 subunit of mitochondrial complex I causes Leigh syndrome. *J. Med. Genet.* **41**:14–17.
9. van den Heuvel, L., et al. 1998. Demonstration of a new pathogenic mutation in human complex I deficiency: a 5-bp duplication in the 18-kD (AQDQ) subunit. *Am. J. Hum. Genet.* **62**:262–268.
10. Triepels, R.H., et al. 1999. Leigh syndrome associated with a mutation in the NDUFS7 (PSST) nuclear encoded subunit of complex I. *Ann. Neurol.* **45**:787–790.
11. Loeffen, J., et al. 1998. The first nuclear-encoded complex I mutation in a patient with Leigh syndrome. *Am. J. Hum. Genet.* **63**:1598–1608.
12. Schuelke, M., et al. 1999. Mutant NDUFV1 subunit of mitochondrial complex I causes leukodystrophy and myoclonic epilepsy. *Nat. Genet.* **21**:260–261.
13. Benit, P., et al. 2003. Genotyping microsatellite DNA markers at putative disease loci in inbred/multiplex families with respiratory chain complex I deficiency allows rapid identification of a novel nonsense mutation (IVS1nt -1) in the NDUFS4 gene in Leigh syndrome. *Hum. Genet.* **112**:563–566.
14. Lebon, S., et al. 2003. Recurrent de novo mitochondrial DNA mutations in respiratory chain deficiency. *J. Med. Genet.* **40**:896–899.
15. McFarland, R., et al. 2004. De novo mutations in the mitochondrial ND3 gene as a cause of infantile mitochondrial encephalopathy and complex I deficiency. *Ann. Neurol.* **55**:58–64.
16. Papa, S., et al. 2002. The NADH: ubiquinone oxidoreductase (complex I) of the mammalian respiratory chain and the cAMP cascade. *J. Bioenerg. Biomembr.* **34**:1–10.
17. Thorburn, D.R. 2004. Mitochondrial disorders: Prevalence, myths and advances. *J. Inherit. Metab. Dis.* **27**:349–362.
18. Kuffner, R., Rohr, A., Schmiede, A., Krull, C., and Schulte, U. 1998. Involvement of two novel chaperones in the assembly of mitochondrial NADH: Ubiquinone oxidoreductase (complex I). *J. Mol. Biol.* **283**:409–417.
19. Janssen, R., Smeitink, J., Smeets, R., and van Den Heuvel, L. 2002. CIA30 complex I assembly factor: a candidate for human complex I deficiency? *Hum. Genet.* **110**:264–270.
20. Brul, S., et al. 1988. Genetic heterogeneity in the cerebrohepatorenal (Zellweger) syndrome and other inherited disorders with a generalized impairment of peroxisomal functions. A study using complementation analysis. *J. Clin. Invest.* **81**:1710–1715.
21. Brown, R.M., and Brown, G.K. 1996. Complementation analysis of systemic cytochrome oxidase deficiency presenting as Leigh syndrome. *J. Inherit. Metab. Dis.* **19**:752–760.
22. Munaro, M., et al. 1997. A single cell complementation class is common to several cases of cytochrome c oxidase-defective Leigh's syndrome. *Hum. Mol. Genet.* **6**:221–228.
23. Reuber, B.E., et al. 1997. Mutations in PEX1 are the most common cause of peroxisome biogenesis disorders. *Nat. Genet.* **17**:445–448.
24. Portsteffen, H., et al. 1997. Human PEX1 is mutated in complementation group 1 of the peroxisome biogenesis disorders. *Nat. Genet.* **17**:449–452.
25. Zhu, Z., et al. 1998. SURF1, encoding a factor involved in the biogenesis of cytochrome c oxidase, is mutated in Leigh syndrome. *Nat. Genet.* **20**:337–343.
26. Tiranti, V., et al. 1998. Mutations of SURF-1 in Leigh disease associated with cytochrome c oxidase deficiency. *Am. J. Hum. Genet.* **63**:1609–1621.
27. Bernier, F.P., et al. 2002. Diagnostic criteria for respiratory chain disorders in adults and children. *Neurology.* **59**:1406–1411.
28. Procaccio, V., et al. 1999. Nuclear DNA origin of mitochondrial complex I deficiency in fatal infantile lactic acidosis evidenced by transnuclear complementation of cultured fibroblasts. *J. Clin. Invest.* **104**:83–92.
29. Sykes, B., Leiboff, A., Low-Beer, J., Tetzner, S., and Richards, M. 1995. The origins of the Polynesians: an interpretation from mitochondrial lineage analysis. *Am. J. Hum. Genet.* **57**:1463–1475.
30. Schagger, H., and von Jagow, G. 1991. Blue native electrophoresis for isolation of membrane protein complexes in enzymatically active form. *Anal. Biochem.* **199**:223–231.
31. Lorain, S., Lecluse, Y., Scamps, C., Mattei, M.G., and Lipinski, M. 2001. Identification of human and mouse HIRA-interacting protein-5 (HIRIP5), two mammalian representatives in a family of phylogenetically conserved proteins with a role in the biogenesis of Fe/S proteins. *Biochim. Biophys. Acta.* **1517**:376–383.
32. Kirby, D.M., et al. 2003. Low mutant load of mitochondrial DNA G13513A mutation can cause Leigh's disease. *Ann. Neurol.* **54**:473–478.
33. Kirby, D.M., et al. 2004. Mutations of the mitochondrial *ND1* gene as a cause of MELAS. *J. Med. Genet.* In press.
34. Schulte, U. 2001. Biogenesis of respiratory complex I. *J. Bioenerg. Biomembr.* **33**:205–212.
35. Cardol, P., Matagne, R.F., and Remacle, C. 2002. Impact of mutations affecting ND mitochondria-encoded subunits on the activity and assembly of complex I in Chlamydomonas. Implication for the structural organization of the enzyme. *J. Mol. Biol.* **319**:1211–1221.
36. Antonicka, H., et al. 2003. Identification and characterization of a common set of complex I assembly intermediates in mitochondria from patients with complex I deficiency. *J. Biol. Chem.* **278**:43081–43088.
37. Rahman, S., et al. 1996. Leigh syndrome: clinical features and biochemical and DNA abnormalities. *Ann. Neurol.* **39**:343–351.
38. Cuthbert, A.P., et al. 1995. Construction and characterization of a highly stable human: rodent monochromosomal hybrid panel for genetic complementation and genome mapping studies. *Cytogenet. Cell Genet.* **71**:68–76.
39. Lamande, S.R., et al. 1998. Reduced collagen VI causes Bethlem myopathy: a heterozygous COL6A1 nonsense mutation results in mRNA decay and functional haploinsufficiency. *Hum. Mol. Genet.* **7**:981–989.
40. Taylor, R.W., Taylor, G.A., Durham, S.E., and Turnbull, D.M. 2001. The determination of complete human mitochondrial DNA sequences in single cells: implications for the study of somatic mitochondrial DNA point mutations. *Nucleic Acids Res.* **29**:E74.
41. Lonnstedt, I., and Speed, T.P. 2002. Replicated microarray data. *Statistica Sinica.* **12**:31–46.